



Cite this: *Green Chem.*, 2020, **22**, 7989

## Cleavage of ethers and demethylation of lignin in acidic concentrated lithium bromide (ACLB) solution†

Zheng Li, <sup>a</sup> Eka Sutandar,<sup>a</sup> Thomas Goihl,<sup>a</sup> Xiao Zhang <sup>b</sup> and Xuejun Pan \*<sup>a</sup>

The methoxyl group is the most abundant functional group of lignin and affects the properties, reactivity, and application of lignin. Efficient demethylation is always of interest in the area of lignin chemistry and application. This study demonstrated a new method for cleaving ether compounds and demethylating lignin in acidic concentrated lithium bromide (ACLB) solution under mild conditions. It was found that the ACLB system could universally cleave ether compounds except for diaryl ethers. The study on lignin model compounds (creosol, syringol, and 1,2,3-trimethoxybenzene) verified that ACLB could demethylate them to corresponding phenols. Four real lignin samples produced from various sources by different methods were also efficiently demethylated by 69–82% in ACLB. The lignin demethylation resulted in more phenolic hydroxyl groups, which benefits some downstream applications of lignin. This study also provided new insights into the cleavage of the ether bonds in lignin. In addition to the methyl–aryl ether bond, ACLB could cleave other ether bonds of lignin in  $\beta$ -O-4,  $\beta$ -5, and  $\beta$ - $\beta$  structures except for the 4-O-5 bond in the diphenyl structure. The ether bonds were cleaved *via* the  $S_N2$  substitution except for the  $\beta$ -O-4 bond, which was primarily cleaved *via* the benzyl cation and enol ether intermediates, leading to Hibbert's ketones. Some of the  $\beta$ -O-4 structures were transformed into benzodioxane (BD) structures, which were stable in the ACLB system.

Received 27th July 2020,  
Accepted 9th October 2020

DOI: 10.1039/d0gc02581j

rsc.li/greenchem

## Introduction

The valorization of lignin to high-value products has been challenging due to the complicated structure and unsatisfactory reactivity of lignin, which is built up from the C9 units including coniferyl alcohol (**G**) with one methoxyl group, sinapyl alcohol (**S**) units with two methoxyl groups, and *p*-coumaryl alcohol (**H**) with no methoxyl substituent.<sup>1–4</sup> The content and structure of lignin vary among different taxonomic groups, cell types, and even layers of the plant cell wall and are greatly influenced by developmental and environmental cues.<sup>3</sup> With few exceptions, angiosperm (hardwood) lignin typically consists of **S** and **G** units with a trace of **H** units, while gymnosperm (softwood) lignin contains almost exclusively **G** units along with a small amount of **S** and **H** units.<sup>5,6</sup> Herbage (grass) lignin usually possesses more **H** units than wood lignin.<sup>3</sup> These units are interlinked mainly *via* carbon–carbon (C–C) and ether (C–O–C) bonds,

including 5–5 (biphenyl),  $\beta$ -5 (phenylcoumaran),  $\beta$ - $\beta$  (resinol), and  $\beta$ -1 (1,2-diarylpropane), and  $\beta$ -O-4 ( $\beta$ -aryl ether) and 4-O-5 (diphenyl ether), respectively.<sup>4</sup> When lignin is isolated from the plant cell wall, its structure changes, dependent on the chemicals and reaction conditions involved in the lignin isolation. For example, milled wood lignin (isolated by finely grinding the plant cell wall followed by solvent extraction) and enzymatic lignin (isolated by enzymatic removal of carbohydrates followed by purification) maintain lignin structures relatively intact, while the lignins isolated by the chemical processes (such as pulping and pretreatment) using alkalis, acids, and organic solvents at high temperature lose most of their  $\beta$ -O-4 bonds and obtain new condensation structures (C–C linkages).<sup>7–10</sup>

Lignin has multiple functional groups including methoxyl, aromatic hydroxyl, aliphatic hydroxyl, carbonyl, and carboxyl groups, which affect the properties and reactivity of lignin. The quantity of the functional groups is determined by the source and isolation method and condition of the lignin. The methoxyl group (OMe) is the most abundant function group in lignin, counting for up to 24% in lignin and 6% in whole wood. Methoxyl groups are critical to the properties, reactivity, and application of lignin. For example, since lignin units without methoxyl groups are easier to couple each other to form interunit C–C bonds,<sup>11</sup> the lignin with a high content of methoxyl

<sup>a</sup>Department of Biological Systems Engineering, University of Wisconsin-Madison, 460 Henry Mall, Madison, WI 53706, USA. E-mail: xpan@wisc.edu

<sup>b</sup>School of Chemical Engineering and Bioengineering, Washington State University, 2710 University Drive, Richland, WA 99354, USA

†Electronic supplementary information (ESI) available. See DOI: 10.1039/d0gc02581j



groups, such as hardwood lignin, usually has a low density of interunit C–C linkages, and such lignin is easier to be depolymerized.<sup>12</sup> Fewer C–C linkages lead to the higher mobility of lignin molecules and therefore lower glass transition temperature.<sup>13</sup> Methoxyl groups help stabilize phenoxyl radicals, which contributes to the antioxidant capacity of lignin.<sup>14,15</sup> On the other hand, demethylation (converting methoxyl to a phenolic hydroxyl group) can improve lignin reactivity toward cross-linking, degradation, and other modifications. For example, demethylated lignin had a higher reactivity in lignin-based phenolic resins, resulting in a stronger binding strength and a lower formaldehyde emission.<sup>16–20</sup> Demethylated lignin showed a higher adsorption capacity of heavy metals.<sup>21</sup> It was reported that the demethylation favored the opening of the lignin benzene ring during biological degradation<sup>22–24</sup> and could promote the Fenton reaction in lignin biodegradation by rot fungi.<sup>25</sup> Demethylated lignin was a more reactive precursor for the production of polyphenols.<sup>26</sup> The methyl group cleaved from lignin could be selectively converted to acetic acid over RuCl<sub>3</sub> in the presence of CO and H<sub>2</sub>O.<sup>27</sup> Besides, demethylation is a key step to produce dimethyl sulfoxide from lignin.<sup>28,29</sup>

The demethylation of lignin, which cleaves the stable ether bond between the benzene ring and methyl group, usually requires special reagents (mostly toxic, expensive, and unstable) and/or harsh conditions (such as high temperature and strong acidity).<sup>30,31</sup> For example, molten pyridine hydrochloride is a classic reagent for cleaving the aryl methyl ether at a temperature as high as 200 °C.<sup>32</sup> Concentrated HBr and HI can selectively demethylate lignin, which have been used for quantitating the methoxyl group of lignin.<sup>26,33–35</sup> Iodic reagents such as iodocyclohexane and trimethylsilyl iodide are also effective for the demethylation.<sup>36–39</sup> Besides, BBr<sub>3</sub> and AlI<sub>3</sub> can demethylate lignin and lignin model compounds at or below room temperature.<sup>40–42</sup>

The present work thus aimed at developing a new method for lignin demethylation under mild conditions using an acidic concentrated lithium bromide (ACLB) solution. This system was first introduced in our previous studies for the fractionation and saccharification of raw biomass and quantitation of lignin.<sup>43,44</sup> With low-concentration acid (0.04–0.3 mol L<sup>-1</sup> or 0.1–1 wt% HCl or HBr) as a catalyst, the ACLB system was able to effectively cleave β-aryl ether (β-O-4), and NMR evidence indicated that the α-O-4 ether bond in phenylcoumaran (β-5) and the α-O-γ ether bond in resinol (β-β) were partially cleaved.<sup>44–46</sup> It was confirmed that the cleavage of the β-O-4 ether bond was completed *via* the Br<sup>-</sup> and H<sup>+</sup> promoted benzyl cation and enol ether intermediates, leading to the formation of Hibbert's ketones, and some of the benzyl cations transformed to a benzodioxane (BD) structure.<sup>46</sup> However, the mechanisms of BD formation and the cleavage of the ether bonds in phenylcoumaran and resinol had not been clearly and sufficiently addressed.

Inspired by the observations above from the previous studies that the ACLB system can cleave the ether bonds in lignin, we hypothesized that the ACLB system could be developed into a new method for cleaving regular ether compounds under milder conditions. In particular, we were interested in

establishing a new method based on the ACLB system for lignin demethylation to produce phenolic hydroxyl-rich lignin for downstream lignin application. In addition, we wanted to revisit the cleaving mechanisms of the ether bonds of lignin in the ACLB system. Herein, we first tested the ACLB system for cleaving different types of ether compounds and demethylating lignin model compounds with different numbers of methoxyl groups. We then carefully investigated the demethylation of a real lignin, ethanol poplar lignin (EPL), in the ACLB system. Three other real lignin samples including hardwood kraft lignin (HKL), corn stover lignin (CSL), and ethanol lodgepole pine lignin (ELPPL) were also tested to verify the applicability of the ACLB system for lignin demethylation. The mechanisms of the cleavage of the ether bonds in lignin and the formation of BD in the ACLB system were revisited and clarified based on the new findings from the present study.

## Experimental

### Materials

All chemicals were used as received. Creosol (98%), syringol (99%), pyrogallol (99%), and pyridine (99%) were purchased from Alfa Aesar. 1,2,3-Trimethoxybenzene (98%) was purchased from Frontier Scientific. LiBr (99%), Na<sub>2</sub>SO<sub>4</sub> (99%), NaCl (99%) and deuterated DMSO (99%) were purchased from Sigma-Aldrich. Tetrahydrofuran (THF, HPLC grade) was purchased from Fisher Scientific. HBr (48%) was provided by Honeywell. HCl (37%) was provided by Mecron. Acetic anhydride was purchased from MP Biochemicals. 4-Nitrobenzaldehyde (98%) was purchased from Ark Pharm. Deuterated chloroform (99.75%, contained 1 v/v% of TMS) was from Acros Organics. Hardwood Kraft lignin (HKL) was supplied by Westvaco (New York, NY). Corn stover lignin (CSL) was extracted using NaOH from the corn stover residue after furfural production from hemicellulose followed by enzymatic hydrolysis of cellulose to glucose for ethanol. The extracted CSL was precipitated with acid, washed to neutral, and then freeze-dried. The preparation and properties of ethanol lodgepole pine lignin (ELPPL) and ethanol poplar lignin (EPL) were described in our previous studies.<sup>14,47</sup>

### Experimental approaches

**Cleavage of ether compounds and demethylation of lignin model compounds in the ACLB system.** In a typical reaction, 6.1 g LiBr and 3.9 g water were mixed in a round-bottomed glass flask with a PTFE stirring bar and a reflux condenser. The mixture was stirred for 2 min until LiBr was fully dissolved to give a colorless solution. An ether or lignin model compound (0.1 g) was added to the solution followed by the addition of 1 mL concentrated HBr (1.48 g, 48%). The final LiBr concentration was 53%. The mixture was then heated in an oil bath to the reaction temperature. After the reaction, the mixture was cooled in ice water and extracted with ethyl acetate (10 mL for 3 times). About 10 mL brine was added to the water phase to increase the extraction efficiency. The organic phases were combined and washed with 10 mL brine



to remove the remaining HBr in the organic phase, and then weighed and stored for further analysis.

**Demethylation of lignin in the ACLB system.** In a typical reaction, 6.1 g LiBr and 3.9 g water were mixed in a round-bottomed glass flask with a PTFE stirring bar and a reflux condenser. The mixture was stirred for 2 min until LiBr was fully dissolved to give a colorless solution. The lignin sample (0.5 g) was added to the solution followed by the addition of 1 mL concentrated HBr (1.48 g, 48%). The final LiBr concentration was 53%. The mixture was then heated in an oil bath to the reaction temperature. For reactions conducted at high temperature (120 °C), lignin and ACLB were introduced into a sealed reactor with a PTFE liner and a stirring bar. The reactor was then heated to the temperature within 30 min in an oil bath. After the reaction, the mixture was cooled in ice water and filtered on a glass Büchner funnel. The collected demethylated lignin was washed with deionized water until the filtrate was neutral. The solid was then dried in a lyophilizer overnight and weighed for calculating mass recovery.

The theoretical mass loss induced by the demethylation of  $\text{ArOCH}_3$  to  $\text{ArOH}$  was calculated using eqn (1).

$$\text{Mass loss (\%)} = (c_{\text{Original OMe}} - c_{\text{OMe after demethylation}}) \times (31 - 17) \text{ g mol}^{-1} \div 1000 \times 100\% \quad (1)$$

where  $c_{\text{original OMe}}$  is the OMe content in original lignin ( $\text{mmol g}^{-1}$ ) calculated by the integration of the corresponding  $^1\text{H}$  NMR signal;  $c_{\text{OMe after demethylation}}$  is the OMe content in the demethylated lignin ( $\text{mmol g}^{-1}$  lignin) that was also calculated by  $^1\text{H}$  NMR signals; 31 is the formula weight of the OMe group; 17 is the formula weight of the OH group.

**GC-MS analysis.** The demethylation products from model compounds were analyzed on a Shimadzu GC2010-QP2010S GC-MS instrument equipped with an Rtx-5MS column ( $30.0 \text{ m} \times 250 \mu\text{m} \times 0.25 \mu\text{m}$ ). The following temperature program was used in the analysis: at 40 °C for 2 min, heated to 220 °C at a rate of 10 °C per min, and then at 220 °C for 2 min. The carrier gas was He at a flow rate of  $1.34 \text{ mL min}^{-1}$ , and the split ratio was 1:20. Mass spectra ranging from  $m/z = 50$ –550 were obtained using electron impact ionization (EI). The concentration of the products was calculated using the external standard method in the software of GC-MS. The yield of the products was calculated using eqn (2).

$$Y_{\text{product}} = \frac{(c_{\text{product}} \times m_{\text{organic phase}}) / M_{\text{product}}}{m_{\text{substrate}} / M_{\text{substrate}}} \times 100\% \quad (2)$$

where  $Y_{\text{product}}$  is the yield of the product;  $c_{\text{product}}$  is the GC-MS detected concentration of the product in the organic phase;  $m_{\text{organic phase}}$  is the mass of ethyl acetate solution after the extraction;  $M_{\text{product}}$  is the molecular weight of the product;  $m_{\text{substrate}}$  is the mass of the starting material;  $M_{\text{substrate}}$  is the molecular weight of the starting material. The external method was also used for the quantitation of anisole, phenetole, diphenyl ether, and their demethylation/dealkylation products.

**GC analysis.** The semi-quantitation of diethyl ether, dibutyl ether, THF, dioxane, and their dealkylation products was con-

ducted on a Shimadzu GC2014 GC instrument equipped with a flame ionization detector and an Rtx-5 column. The following temperature program was used in the analysis: at 40 °C for 2 min, heated to 220 °C at a rate of 10 °C per min, and then at 220 °C for 2 min. The carrier gas was  $\text{N}_2$  at a flow rate of  $1.0 \text{ mL min}^{-1}$ , and the split ratio was 1:20. The concentration of a product was semi-quantitated by the internal standard method with hexane as an internal standard based on the following eqn (3):

$$c_{\text{product}} = \frac{S_{\text{product}} \times c_{\text{hexane}}}{S_{\text{hexane}}} \quad (3)$$

where  $c_{\text{product}}$  is the concentration of the product in ethyl acetate after the extraction;  $S_{\text{product}}$  is the signal area detected by GC;  $c_{\text{hexane}}$  is the concentration of hexane in ethyl acetate after the extraction;  $S_{\text{hexane}}$  is the signal area of hexane detected by GC. The conversion and yield of diethyl ether, dibutyl ether, THF, dioxane, and their dealkylation products were calculated using the same method.

**NMR analysis.** The original and demethylated lignin samples were acetylated before NMR analysis to convert the  $\text{ArOH}$  and  $\text{AlkOH}$  groups to phenolic and alkyl acetates, respectively. In brief, 0.1 g lignin sample and 1 mL pyridine were mixed in a glass vial with a PTFE stirring bar. The mixture was stirred for 10 min, and lignin was fully dissolved in pyridine, giving a viscous dark liquid. Acetic anhydride (1 mL) was then added dropwise to the vial. The mixture was stirred at room temperature in the dark for 72 h. After acetylation, the black oily mixture was added dropwise to dilute HCl (1 mL concentrated HCl in 100 mL water). The solution was then filtered on a glass Büchner funnel and a yellow to brown solid was collected. The acetylated lignin sample was then dried in a lyophilizer overnight and stored for further analysis.

The contents of OMe,  $\text{ArOH}$ , and  $\text{AlkOH}$  in lignin were quantitated using  $^1\text{H}$  NMR with 4-nitrobenzaldehyde as an internal standard. In brief, about 5–10 mg 4-nitrobenzaldehyde and 10–15 mg acetylated lignin were fully dissolved in 0.5 mL  $\text{CDCl}_3$ .  $^1\text{H}$  NMR spectra were recorded on a Bruker AV III 500 MHz spectrometer (Billerica, MA) with an operating frequency of 500 MHz. The data were processed using MestReNova desktop NMR data processing software (version 11.0.4). The phase and baseline in all the spectra were corrected automatically before integration. The contents of OMe,  $\text{ArOH}$ , and  $\text{AlkOH}$  were calculated using eqn (4)–(6):<sup>14</sup>

$$F_{\text{-OMe}} \text{ (mmol g}^{-1} \text{ of lignin)} = \frac{\frac{I_{4.10-3.10 \text{ ppm}}}{3} \times \frac{2}{I_{4\text{-NBA at } 8.40 \text{ ppm}}} \times \frac{m_{4\text{-NBA}}}{151} \times 1000}{m_{\text{lignin}} - \frac{I_{2.50-1.70 \text{ ppm}}}{3} \times \frac{2}{I_{4\text{-NBA at } 8.40 \text{ ppm}}} \times \frac{m_{4\text{-NBA}}}{151}} \times 42 \quad (4)$$

$$F_{\text{ArOH}} \text{ (mmol g}^{-1} \text{ of lignin)} = \frac{\frac{I_{2.50-2.17 \text{ ppm}}}{3} \times \frac{2}{I_{4\text{-NBA at } 8.40 \text{ ppm}}} \times \frac{m_{4\text{-NBA}}}{151} \times 1000}{m_{\text{lignin}} - \frac{I_{2.50-1.70 \text{ ppm}}}{3} \times \frac{2}{I_{4\text{-NBA at } 8.40 \text{ ppm}}} \times \frac{m_{4\text{-NBA}}}{151}} \times 42 \quad (5)$$



$$F_{\text{AlkOH}}(\text{mmol g}^{-1} \text{ of lignin}) = \frac{\frac{I_{2.17-1.70 \text{ ppm}}}{3} \times \frac{2}{I_{4\text{-NBA at } 8.40 \text{ ppm}}} \times \frac{m_{4\text{-NBA}}}{151} \times 1000}{m_{\text{lignin}} - \frac{I_{2.50-1.70 \text{ ppm}}}{3} \times \frac{2}{I_{4\text{-NBA at } 8.40 \text{ ppm}}} \times \frac{m_{4\text{-NBA}}}{151}} \times 42 \quad (6)$$

where  $F$  is the content of the functional groups;  $I$  is the integration of protons of the functional groups ( $\delta$  4.10–3.10 ppm for MeO,  $\delta$  2.50–2.17 ppm for the acetyl group corresponding to ArOH, and  $\delta$  2.17–1.70 ppm for the acetyl group corresponding to AlkOH, respectively); 3 is the number of protons of acetyl and methoxyl groups; 2 is the number of protons of the signal of 4-nitrobenzaldehyde at  $\delta$  8.44–8.34 ppm;  $m_{4\text{-NBA}}$  is the weight of 4-nitrobenzaldehyde; 151 is the formula weight of 4-nitrobenzaldehyde;  $m_{\text{lignin}}$  is the weight of the acetylated lignin (mg);  $I_{2.5-1.7}$  is the integration of protons of total acetyl groups corresponding to ArOH and AlkOH ( $\delta$  2.50–1.70 ppm); 42 is the formula weight of acetyl group minus one (43 – 1).

For the collection of HSQC spectra, about 50 mg unacetylated lignin was fully dissolved in 0.5 mL DMSO- $D_6$ . The samples were analyzed on a Bruker AV III 500 MHz spectrometer equipped with a DCH ( $^{13}\text{C}$ -optimized) cryoprobe (Billerica, MA). The test was conducted at 25 °C with Bruker's standard `hsqcetgpsisp 2.2` pulse program (acquisition times 200 ms and 8 ms in  $^1\text{H}$  and  $^{13}\text{C}$  dimensions, inter-scan relaxation delay 1 s). Data were analyzed using Bruker's Topspin 4.0.8 software.

**GPC analysis.** Average molecular weights ( $M_n$  and  $M_w$ ) of the acetylated lignin samples were estimated by GPC on an ICS-3000 system (Dionex, Sunnyvale, CA) with three 300 mm  $\times$  7.8 mm i.d. Phenogel 5U columns (10 000, 500, and 50 Å) and a 50 mm  $\times$  7.8 mm i.d. Phenogel 5U guard column (Phenomenex, Torrance, CA). Lignin acetate (about 3 mg) was dissolved in 5 mL HPLC grade tetrahydrofuran (THF) without a stabilizer, and about 500  $\mu\text{L}$  the solution was injected into the GPC system. THF was used as the eluent at a flow rate of 1 mL  $\text{min}^{-1}$ . The column temperature was 30 °C. Polystyrene standards were used for calibration. Lignin samples and polystyrene standards were detected using a variable wavelength detector (VWD) at 280 and 254 nm, respectively.

**SEM-EDS analysis.** Field emission scanning electron microscopy (FESEM, Leo Co., Oberkochen, Germany) coupled with energy dispersive spectroscopy (EDS) was used to detect bromine in demethylated lignin in the ACLB. The lignin sample was coated with 10 nm of gold. The accelerating voltage was 15.0 kV.

## Results and discussion

### Cleavage of ether compounds in the ACLB system

Ethers are not commonly reactive toward many reactions, except for highly strained cyclic ethers (oxirane and oxetane). A textbook method for cleaving an ether is to heat it with concentrated HBr or HI because they are sufficiently acidic to protonate the ether, while bromide and iodide are good nucleophiles for the substitution. Specifically, the protonation of the

ether oxygen forms an oxonium ion, and then the nucleophile ( $\text{Br}^-$  or  $\text{I}^-$ ) attacks the backside of the electrophilic  $\alpha$ -carbon of the ether *via* the  $\text{S}_{\text{N}}2$  mechanism, leading to the cleavage of the ether bond.

To investigate the capability of the ACLB to cleave ethers, different ether compounds including linear and cyclic ethers were treated. As summarized in Table 1, all the ether compounds except diphenyl ether could be cleaved in the ACLB. The conversion and product yield depended on the structure of the ethers and reaction conditions. The cleavage of an ether *via* the  $\text{S}_{\text{N}}2$  substitution by  $\text{Br}^-$  yields an alcohol and a bromide. The alcohol can further react with  $\text{Br}^-$  to give another bromide, while the bromide intermediate can be further hydrolyzed into another alcohol. Both the alcohol and the bromide were detected in the products. The yield of the products listed in Table 1 (entries 1–7) is the combined yield of the alcohol and the bromide.

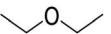
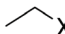
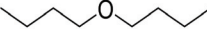

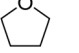
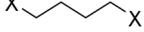
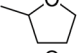
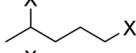
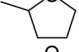
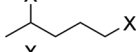
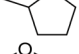
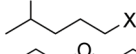
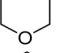
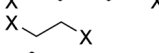
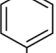
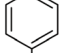
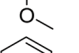
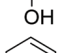
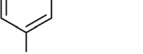
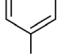
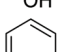
Diethyl ether and dibutyl ether were both cleaved to give ethanol/bromoethane and butanol/bromobutane as products, respectively (entries 1 and 2 in Table 1). Because of a larger steric hindrance at the  $\alpha$ -carbon for the  $\text{S}_{\text{N}}2$  substitution, the debutylation of dibutyl ether was slower than the deethylation of diethyl ether.

Cyclic ethers are easier to be cleaved than linear ethers because of the high strain of the former. For example, tetrahydrofuran (THF) was ring-opened to 1,4-butanediol and its bromides very rapidly even at room temperature (Table 1, entry 3), which was in agreement with the previous observation that THF was very reactive to undergo polymerization in the presence of Brønsted or Lewis acid.<sup>48,49</sup> Dioxane was much more stable than THF in ACLB (entry 7 in Table 1) because the six-membered ring of dioxane is less strained than the five-membered ring of THF. A similar result was observed in other acidic systems as well.<sup>49,50</sup> The cleavage of the first ether bond of dioxane occurred faster than the second one, and the yield of the product from the first step (70%) was much higher than that from the second step (25%). However, the cleavage of dioxane was easier than diethyl and dibutyl ethers, since the conversion and product yield of dioxane were higher than those of the linear ethers under the same conditions, as shown in Table 1 (entry 7 *vs.* entries 1 and 2).

When the steric hindrance at the  $\alpha$ -carbon is large, the ether cleavage becomes slower and more difficult. For the  $\text{S}_{\text{N}}2$  substitution reactions, the relative rates are in the order of methyl ( $\text{CH}_3^-$ ) > primary carbon ( $\text{RCH}_2^-$ ) > secondary carbon ( $\text{R}_2\text{CH}^-$ )  $\gg$  tertiary carbon ( $\text{R}_3\text{C}^-$ ). For example, 2-methyl THF (entry 4 in Table 1) was cleaved in the ACLB at room temperature, but the relative rate was much lower, compared with THF (entry 3 in Table 1), because one of the  $\alpha$ -carbon (C2) of 2-methyl THF is a secondary carbon. Increasing the severity of reaction conditions, such as acidity, can promote the reaction. For example, with increasing HBr concentration from 0.18 wt% to 1.3 wt% and 6 wt%, the conversion of 2-methyl THF at room temperature increased from 19% to 39% and 75%, and the yield of the products from 3.4% to 18% and 65%, respectively.



Table 1 Cleavage of ethers in the ACLB system. X = OH or Br

Entry	Substrate	Conversion (%)	Target product	Yield (%)
1		ND <sup>a</sup>		45 <sup>a</sup>
2		15		30
3 <sup>b</sup>		100		>95
4 <sup>c</sup>		19		3.4
5 <sup>d</sup>		39		18
6 <sup>e</sup>		75		65
7		83		70
8		47		25
9		35		38
10 <sup>f</sup>		<5		17
				ND

ND – not determined. Reaction conditions (unless indicated separately): 0.1 g substrate, 10 g 53 wt% LiBr with 6 wt% HBr, 100 °C, and 4 h. <sup>a</sup> Not accurate due to the mass loss of the volatile reactant and products. <sup>b</sup> Room temperature and 1 h. <sup>c</sup> 0.18 wt% HBr, room temperature, and 2 h. <sup>d</sup> 1.3 wt% HBr, room temperature, and 2 h. <sup>e</sup> 6 wt% HBr, room temperature, and 2 h. <sup>f</sup> 6 wt% HBr, 120 °C, and 4 h.

Alkyl aryl ethers were cleaved as well in the ACLB, generating a phenol and an alkyl bromide. For example, anisole was cleaved to phenol and bromomethane under the tested conditions (entry 8 in Table 1). The cleavage of phenetole to phenol and bromoethane was slower than anisole because of the larger steric hindrance of the primary  $\alpha$ -carbon in the ethyl side of phenetole (entry 9 in Table 1). The alkyl aryl ether can only be cleaved from the alkyl side *via* dealkylation because the  $sp^2$  hybridized carbon atom bonded to ether oxygen on the benzene ring cannot undergo the  $S_N2$  substitution.

Diphenyl ether was stable in ACLB (entry 10 in Table 1) even at a higher temperature due to its high bond dissociation energy (314 kJ mol<sup>-1</sup>).<sup>51,52</sup> Generally, the cleavage of the diphenyl ether is very hard without the assistance of hydrogenation. For the same reason ( $sp^2$  hybridized carbon on benzene ring), the ether bond in diphenyl ether cannot be cleaved *via* the  $S_N2$  mechanism. This result suggests that the ether bond of the 4-O-5 linkage in lignin should be stable in the ACLB system.

#### Demethylation of lignin model compounds in the ACLB system

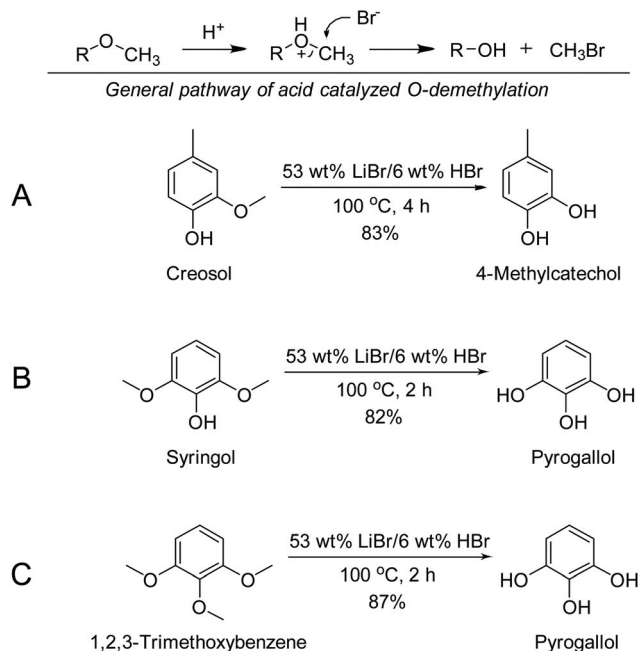
With the results of cleaving the ether compounds above, lignin model compounds with methoxyl group(s) were studied for the demethylation in ACLB. 2-Methoxy-4-methylphenol (creosol) was chosen as a G type lignin model compound. HBr was used

as an acid catalyst, so the ACLB system can be compared with the concentrated HBr system, which is a classic method for ether cleavage. The demethylation mechanism is shown in Scheme 1 (top).

The concentrated HBr system (48 wt%) was first examined for the demethylation of creosol. The concentrated HBr was able to demethylate creosol but required a higher temperature and longer time than the ACLB, as shown in Table 2 (entry 1 *vs.* entries 6 and 7). Besides, the concentrated HBr had a lower yield of 4-methylcatechol and more condensation compounds (black humin-like precipitates), suggesting that ACLB had better selectivity than the concentrated HBr. Differently, 6% HBr in water was unable to demethylate creosol because the acidity and Br<sup>-</sup> concentration were too low to effectively protonate and cleave the ether bond, respectively (entry 2 in Table 2). Similarly, creosol was not demethylated in 61 wt% LiBr in the absence of acid after 20 h treatment (entry 3 in Table 2) because protonation of the ether oxygen by H<sup>+</sup> is a prerequisite to cleave the ether bond by bromide as a nucleophile *via*  $S_N2$  substitution.

As expected, creosol was effectively demethylated in ACLB. For example, creosol was completely converted in 53% and 61% LiBr solutions with 6 wt% HBr at 100 °C, yielding >80% 4-methylcatechol (Scheme 1A and entries 6, 7 in Table 2). The results under other conditions (temperature, acid concen-





**Scheme 1** Demethylation of creosol, 2,6-dimethoxyphenol, and 1,2,3-trimethoxybenzene in the ACLB system.

tration, and acid type) are available in Table S1.† Why low-concentration acid (e.g., 6% HBr) can protonate the ether bond is because the acidity of HBr is enhanced in the concentrated LiBr solution. When highly oxophilic  $\text{Li}^+$  coordinates tightly with  $\text{H}_2\text{O}$  molecules, the  $\text{H}^+$  is less hydrated and has high freedom in the solution, which enhances the acidity of the acid, compared with that in the water at the same acid concentration.<sup>53</sup> Meanwhile, without coordination with water, high-concentration  $\text{Br}^-$  is naked in the solution and freely available for the  $\text{S}_{\text{N}}2$  substitution to cleave the ether bond.<sup>43,54</sup> These are the reasons why creosol was rapidly and effectively demethylated in the concentrated LiBr solutions at a low acid concentration.

The results in Table 2 (entries 4–7) indicate that LiBr concentration is a crucial factor affecting the demethylation. No

demethylation occurred at 40% LiBr concentration (entry 4), apparently due to the insufficient acidity and  $\text{Br}^-$  concentration in the dilute LiBr solution, while 28% demethylation was completed at 47% LiBr concentration (entry 5). Increasing the LiBr concentration to 53% yielded 83% 4-methylcatechol (entry 6). However, further increasing LiBr concentration to 61% did not show a positive effect on the demethylation (entry 7).

When LiBr was replaced by NaBr or KBr, a much lower demethylation rate was observed (entries 8 and 9 in Table 2). Since the solubility of NaBr and KBr was lower and the molecular weight was higher than that of LiBr, the concentration of  $\text{Br}^-$  (the nucleophile for the  $\text{S}_{\text{N}}2$  substitution) is lower in NaBr and KBr solutions than in LiBr solution. Another more important reason is that the lower charge density of  $\text{Na}^+$  and  $\text{K}^+$  because of their larger size makes them have a lower oxophilicity than  $\text{Li}^+$ . Therefore, the coordination of  $\text{Na}^+$  and  $\text{K}^+$  with water is weaker than that of  $\text{Li}^+$ . As a result,  $\text{Br}^-$  has more chances to enter the coordination positions of  $\text{Na}^+$  and  $\text{K}^+$  than those of  $\text{Li}^+$ , which reduces the availability of  $\text{Br}^-$  in the NaBr and KBr solutions for the  $\text{S}_{\text{N}}2$  substitution. For the same reason, the freedom (activity) of  $\text{H}^+$  is reduced in the NaBr and KBr solutions, compared to that in LiBr solution. In other words, NaBr and KBr solutions have a lower acidity and a lower concentration of free  $\text{Br}^-$  than LiBr solution at the same concentration. This is why their performance in the demethylation of creosol follows the order of  $\text{LiBr} > \text{NaBr} > \text{KBr}$ , as shown in Table 2.

HCl as a catalyst gave a comparable yield of 4-methylcatechol in the ACLB with HBr (entry 10 vs. entries 6, 7 in Table 2), indicating that the ether cleaving capability of the ACLB is the unique property of the system because of the enhanced acidity and  $\text{Br}^-$  concentration, independent of the proton source (HBr or HCl). However, the LiCl/HCl system was unable to demethylate creosol (entry 11 in Table 2) due to the lower solubility of LiCl (lower  $\text{Cl}^-$  concentration) and more importantly the much lower nucleophilicity of  $\text{Cl}^-$  than  $\text{Br}^-$  for the  $\text{S}_{\text{N}}2$  substitution.

It is worth mentioning that the demethylation of creosol was much faster than that of anisole in ACLB because the

**Table 2** Demethylation of creosol to 4-methylcatechol in HBr and/or LiBr systems

Entry	Reaction system	Temperature (°C)	Time (h)	Creosol conversion (%)	4-Methylcatechol yield (%)
1 <sup>a</sup>	48 wt% HBr	120	20	100	68
2 <sup>b</sup>	6 wt% HBr	100	4	<5	0
3 <sup>c</sup>	61 wt% LiBr	100	20	33	0
4 <sup>d</sup>	40 wt% LiBr/6 wt% HBr	100	4	25	0
5 <sup>d</sup>	47 wt% LiBr/6 wt% HBr	100	4	31	28
6 <sup>d</sup>	53 wt% LiBr/6 wt% HBr	100	4	100	83
7 <sup>d</sup>	61 wt% LiBr/6 wt% HBr	100	4	100	80
8	48 wt% NaBr/6 wt% HBr	100	4	11	<5
9	40 wt% KBr/6 wt% HBr	100	4	0	0
10	61% LiBr/6 wt% HCl	100	20	99	87
11	46% LiCl/6 wt% HCl	100	4	0	0

<sup>a</sup> 0.5 g creosol in 20 mL 48 wt% HBr. <sup>b</sup> 0.1 g creosol in 10 g water with 1 mL 48 wt% HBr. <sup>c</sup> 0.1 g creosol in 6.1 g LiBr and 3.9 g water. <sup>d</sup> 0.1 g creosol in 10 g aqueous LiBr solution at different concentrations with 1 mL 48 wt% HBr.



hydroxyl group in creosol increases the electron density of the conjugated system, which eases the protonation of methoxy oxygen for the following  $S_N2$  substitution by  $Br^-$ .

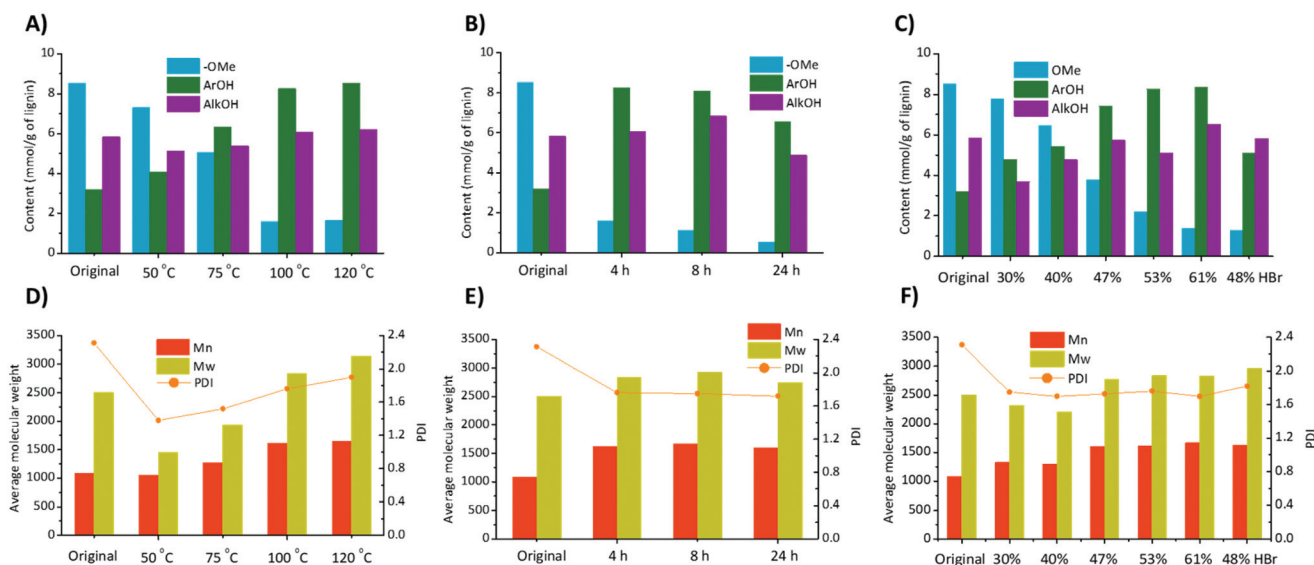
2,6-Dimethoxyphenol (syringol) and 1,2,3-trimethoxybenzene as S type lignin model compounds with more methoxy groups were also investigated for demethylation in the ACLB system (Scheme 1B and C). Both model compounds could be completely demethylated to pyrogallol *via* the intermediates with one or two OMe groups. Besides, it was noted that the hydroxyl-rich intermediates and pyrogallol would condense and form black precipitates with extended reaction.

### Demethylation of ethanol poplar lignin (EPL) in the ACLB system

After proving that ACLB is capable of cleaving aryl methyl ether in the three lignin model compounds above, real lignin (EPL) was tested for demethylation under the same conditions. It was observed that the lignin was well dispersed in the system, and the lignin became darker after the reaction. During the reaction, a thin layer of fine bubbles was observed on the surface of the reaction mixture, which was proved by GC-MS to be bromomethane (b.p. = 3.56 °C) produced from the demethylation. The contents of methoxyl (OMe), aromatic hydroxyl (ArOH), and alkyl hydroxyl groups (AlkOH) of the lignin were quantitated by  $^1H$  NMR, as described in the Experimental section.<sup>14,55</sup> As shown in Fig. 1 (full data available in Table S2<sup>†</sup>), OMe in EPL was efficiently cleaved, resulting in ArOH, which occurred even at 50 °C. Meanwhile, GPC results revealed that the average molecular weights  $M_n$  and  $M_w$  of the lignin decreased from 1080 to 980 and 2500 to 1450, respectively (Fig. 1D), suggesting that lignin depolymerization occurred at a mild temperature in

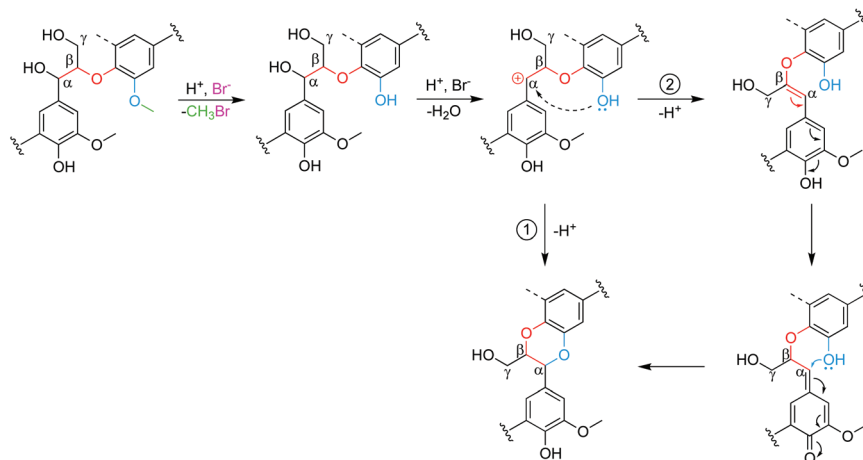
ACLB, which was attributed to the cleavage of the residual  $\beta$ -O-4 bonds. The PDI value decreased as well, indicating that the lignin was homogenized in size due to the depolymerization. Increasing the reaction temperature from 50 °C to 100 °C substantially enhanced the demethylation efficiency, leading to 72% OMe cleavage (to 2.19 mmol  $g^{-1}$ ) with an 81% selectivity to ArOH (8.27 mmol  $g^{-1}$  in total). However, the increased temperature resulted in the repolymerization of lignin, such as the condensation between aromatic C5 or C6 and benzyl cations induced by acid (Scheme S1<sup>†</sup>),<sup>56</sup> and  $M_n$ ,  $M_w$ , and PDI increased from 1050, 1450, and 1.38 to 1620, 2840, and 1.76, respectively. Further elevating temperature to 120 °C brought the cleavage rate of OMe up to 79%. However, the selectivity to ArOH dropped to 78%, and the average molecular weights of the lignin became higher because of promoted repolymerization. To avoid undesired excessive lignin condensation, 100 °C was selected as the working temperature.

A way to redeem the low OMe cleavage at 100 °C is to extend the reaction time. As shown in Fig. 1B, prolonging reaction time from 4 h to 8 h and 24 h increased the cleavage rate of OMe from 72% to 86% and 93%, respectively. However, the increased demethylation did not proportionally turn out as more ArOH but led to reduced ArOH, which was probably attributed to the formation of the benzodioxane (BD) structure, as reported previously.<sup>46</sup> As further discussed in Scheme 2, one ArOH at C3 or C5 is consumed to form the BD structure. The average molecular weights did not change much, suggesting that the repolymerization was not significantly affected by reaction time, although it was very sensitive to reaction temperature (Fig. 1D and E). It was also noted that lignin mass recovery was 79 wt%, which was lower than the reported



**Fig. 1** Demethylation of EPL. (A), (B), and (C) show the quantity of OMe, ArOH, and AlkOH in original and demethylated EPL at different temperatures and reaction times, and in different LiBr concentrations; (D), (E), and (F) show the average molecular weights and polydispersity index (PDI) of original and demethylated EPL at different temperatures, reaction times, and in different LiBr concentrations. Reaction conditions: 0.5 g EPL, 53 wt% LiBr, 6 wt% HBr, 100 °C, and 4 h. All lignin samples were acetylated for NMR and GPC analysis. All reactions were conducted in duplicate except the 30%, 40%, 47%, and 61% LiBr tests (single).





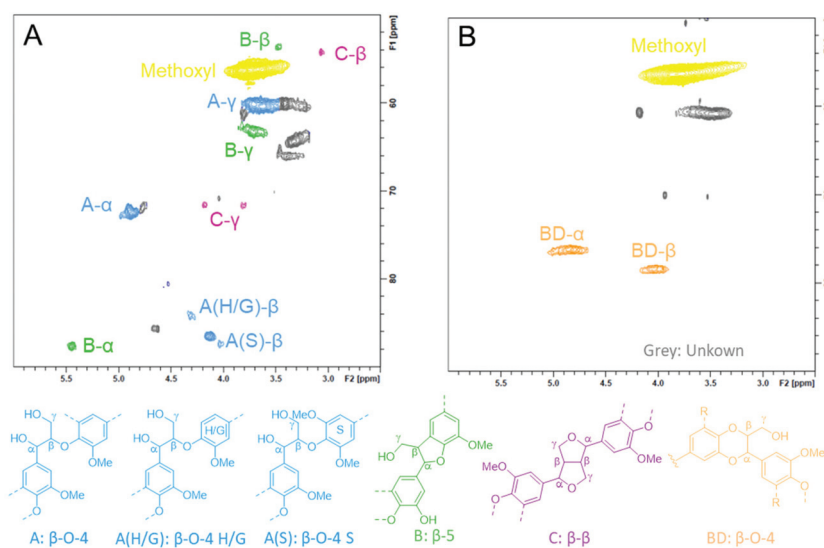
**Scheme 2** Proposed formation mechanism of the BD structure.

mass recovery of 83–94 wt% when lignin was treated under mild conditions (low acid concentration) in ACLB.<sup>45</sup> The additional mass loss was attributed to the demethylation since the elimination of  $\text{CH}_2$  *via* the demethylation could lead to an 8.0 wt% mass loss (calculated from OMe content in EPL).

Since the concentration of LiBr played an important role in the conversion of creosol, it is plausible that the demethylation of lignin is also greatly impacted by LiBr concentration. Therefore, different LiBr concentrations from 30% to 61% were applied for EPL demethylation (Fig. 1C and F). The cleavage degree of OMe and ArOH yield increased when LiBr concentration was increased from 30% to 61%. The average molecular weight also became higher with increased LiBr concentration, suggesting that the acidity of ACLB was likewise enhanced, which promoted the repolymerization of EPL.

To compare the lignin demethylation performance in the ACLB and the traditional HBr system, EPL was also treated in concentrated HBr at 100 °C (Fig. 1C and F). The results indicated that concentrated HBr was able to demethylate EPL as well, and the average molecular weights were nearly identical to those of ACLB treated EPL. The cleavage rate of OMe was 84%, but the selectivity to ArOH was only 22%, much lower than that in the ACLB system, which was probably related to the enhanced lignin condensation in the concentrated HBr. As observed above, creosol and 4-methylcatechol underwent severe condensation in concentrated HBr and generated humin-like precipitates.

To investigate the structural changes to EPL during the demethylation in ACLB, the original and demethylated EPL samples were analyzed by HSQC, as shown in Fig. 2 (aliphatic region), Fig. S3† (aromatic region), and Fig. S4† (lower LiBr concentrations). The original EPL contained abundant OMe groups,



**Fig. 2** Aliphatic regions of the HSQC spectra of original and demethylated EPL in  $\text{DMSO-d}_6$ . (A) Original EPL; (B) demethylated EPL. Reaction conditions: 0.5 g lignin, 53 wt% LiBr, 6% HBr, 100 °C, and 4 h.





$\beta$ -aryl ether **A** (H/G and S units), phenylcumaran **B** ( $\beta$ -5), resinol **C** ( $\beta$ - $\beta$ ), and characteristic *p*-hydroxybenzoate (also see the aromatic region in Fig. S3G<sup>†</sup>). After the demethylation in ACLB, residual OMe groups were still visible, while the characteristic signals of **A**, **B**, and **C** subunits were no longer visible (probably chemically shifted) in the aliphatic region due to the cleavage of the ether bonds in these structures (Fig. 2). The signal of the characteristic *p*-hydroxybenzoate unit, however, did not change after the demethylation (Fig. S3H<sup>†</sup>). Benzodioxane (**BD**) was also observed in the ACLB-treated EPL with 53% LiBr (Fig. 2B), as previously observed when wood was treated in a concentrated LiBr solution.<sup>46</sup> **BD**- $\alpha$  and **BD**- $\beta$  were assigned at  $\delta$ C/ $\delta$ H 76.0/4.81 ppm and 78.4/4.05 ppm, respectively.<sup>57</sup> The **BD** structure was observed in the EPL treated with 40% and 47% LiBr solutions as well, but not that with 30% LiBr (Fig. S4<sup>†</sup>), suggesting that the demethylation of OMe is the precondition of **BD** formation because 30% LiBr cannot efficiently demethylate lignin. The formation of the **BD** structure during the acid-catalyzed lignin depolymerization in the ACLB was reported in our previous study, but the formation mechanism of **BD** was not clearly addressed.<sup>46</sup> Based on the evidence and observation from both the previous<sup>46</sup> and the present studies, the **BD** formation mechanism is elucidated in Scheme 2. The OMe on the benzene ring involved in a  $\beta$ -O-4 linkage is demethylated into ArOH, and meanwhile, the  $\alpha$ -carbon of another lignin unit in the same  $\beta$ -O-4 linkage is cationized by H<sup>+</sup> and/or Br<sup>-</sup>.<sup>46</sup> The ArOH then attacks the electropositive  $\alpha$ -carbon to form the dioxane ring in **BD**.<sup>46,58,59</sup> The ArOH can directly attack the  $\alpha$ -cation to form the dioxane ring (Path 1). Alternatively, the  $\alpha$ -cation is transformed first to enol ether and then to the quinone intermediate, which couples with the ArOH to form the **BD** (Path 2).

**BD** was detected in the EPL treated in the ACLB at a high HBr concentration (6 wt% or about 1.3 mol L<sup>-1</sup>), while the previous observation of **BD** was in the lignins treated at a low acid concentration in the previous study (10–40 mmol L<sup>-1</sup> HCl),<sup>46</sup> indicating that the ether bonds in the **BD** structure were stable and could survive under the severe conditions tested, although dioxane was easily cleaved under the same conditions (entry 7 in Table 1). This can be attributed to the following reasons: (a) the ether bonds in **BD** are not cleavable from the aryl side, as discussed above; and (b) the C $\alpha$  and C $\beta$  of the alkyl side of the ether bonds in **BD** are both secondary carbons, which have higher steric hindrance, in particular, the C $\alpha$  bonded to a benzene ring, to the S<sub>N</sub>2 substitution for cleaving the ether bonds, compared to the primary carbons in dioxane. By this means, **BD** can be treated as a “sealed”  $\beta$ -O-4 structure. Apparently, the formation of **BD** consumed some of the ArOH generated by the demethylation, which explained why ArOH did not increase proportionally with the demethylation degree, as discussed above. Hibbert’s ketone (**HK**) was not detected in the ACLB-treated EPL as in the previous studies,<sup>43,45,46</sup> possibly due to the higher acid concentration used in the present study, which promoted the aldol condensation of the ketone.<sup>46,60</sup>

Although EPL was very well dispersed in the ACLB system, the reaction was still heterogeneous (lignin retained undissolved), so the OMe groups inside lignin particles might be

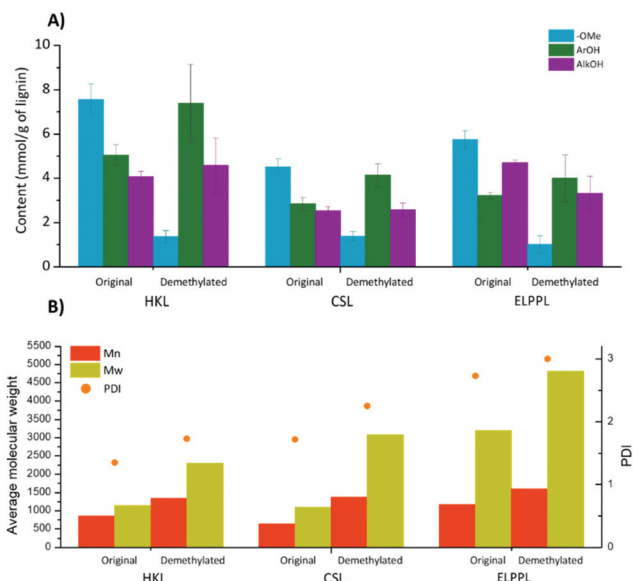
less accessible than those exposed on the surface. To dissolve EPL for a homogeneous reaction, acetic acid, ethanol, and acetone were tested as co-solvents for in the demethylation of EPL (Table S3<sup>†</sup>). All three co-solvents were miscible with the ACLB to give clear solutions at room temperature, and EPL was soluble in the three co-solvent-ACLB systems. It was found that acetic acid and acetone did not significantly affect the demethylation performance, suggesting that lignin could be demethylated efficiently in the ACLB even without dissolving the lignin. However, the lowest ArOH was detected when ethanol was used as a co-solvent (Table S3<sup>†</sup>). This is probably due to the etherification between ethanol and ArOH formed from the demethylation, which was supported by the detection of ethoxy groups in the treated lignin by the HSQC spectrum (Fig. S1D<sup>†</sup>) at  $\delta$ C/ $\delta$ H 64.6/3.44 ppm and 66.3/3.44 ppm. As discussed above, the ethyl-O-aryl bond was more difficult to be cleaved than the methyl-O-aryl bond due to the steric hindrance (Table 1). The re-etherification was probably a reason why both ArOH and AlkOH decreased when the reaction was extended to 24 h in Fig. 1B. Besides, the introduction of ethanol led to much lower average molecular weights of demethylated EPL probably because ethanol prevented the **HK** moieties generated from the cleavage of the  $\beta$ -O-4 bond from condensation. HSQC spectrum revealed that **HK** moieties ( $\delta$ C/ $\delta$ H 45.0/3.61 ppm and 67.6/4.17 ppm in Fig. S1D<sup>†</sup>) were only visible in the demethylated EPL in the ethanol-ACLB. **HK** was stabilized by ethanol probably *via* the acetalization of **HK** or the etherification of the enol form of **HK**. The signal of O-CH<sub>2</sub> was observed in HSQC spectra, which suggested the existence of ethyl ether units (Fig. S1D<sup>†</sup>). The signals of **HK** were also exclusively observed in the aromatic region (Fig. S2D<sup>†</sup>) of the demethylated EPL in the ethanol-ACLB.

### Demethylation of other lignins in the ACLB system

To evaluate the compatibility of the ACLB system, three other lignin samples (HKL, CSL, and ELPL) were treated under the chosen conditions mentioned above for EPL. All three lignin samples were dispersed well in the system and gave homogeneous suspensions. <sup>1</sup>H NMR results confirmed that the OMe content in three original lignins followed the order of HKL > ELPL > CSL since hardwood lignin has more **S** units, while softwood and corn stover lignin contains more **G** and/or **H** units (Fig. S3<sup>†</sup>). As summarized in Fig. 3, after the treatment in the ACLB, the OMe groups in the lignin samples were effectively cleaved, and the ArOH groups increased correspondingly (Fig. 2A). Similar to EPL, *M<sub>n</sub>* and *M<sub>w</sub>* of HKL, CSL, and ELPL all increased after demethylation as a result of repolymerization, which was inevitable in the strongly acidic ACLB system. Different from EPL whose DPI decreased from 2.31 to 1.76, the PDI of HKL, CSL, and ELPL increased from 1.35, 1.72, and 2.73 to 1.73, 2.25, and 3.00, respectively, after the demethylation.

To gain insights into the structural changes to HKL, CSL, and ELPL during the demethylation, their HSQC spectra were recorded, as shown in Fig. 4 (aliphatic region) and Fig. S3<sup>†</sup> (aromatic region). Almost all the ether bonds in **A**, **B**, and **C** structures were cleaved (signals became invisible). Like EPL,





**Fig. 3** Demethylation of HKL, CSL, and ELPL in ACLB. (A) OMe, ArOH, and AlkOH in the lignins quantitated by  $^1\text{H}$  NMR. (B)  $M_n$ ,  $M_w$ , and PDI of the lignins estimated by GPC. Reaction conditions: 0.5 g lignin, 53 wt% LiBr, 6% HBr, 100 °C, and 4 h. All values are the average of triplicated tests (see Table S4† for details).

the demethylation of HKL also led to the formation of **BD** structure (Fig. 4B) as HKL is hardwood lignin with more **S** units (Fig. S3B†). However, **BD** was not detected in the demethylated CSL and ELPL. As shown in Scheme 2, the formation of **BD** requires the presence of the ArOH generated from demethylation and the rotation of the benzene ring for the ArOH to attack the  $\alpha$ -carbon of another lignin unit. Hardwood lignin has more **S** units, which have more OMe and fewer interunit C–C linkages and thereby better mobility for the rotation to facilitate the formation of **BD** formation, than softwood and grass lignin. This is why **BD** was detected in the demethylated HKL but not CSL and ELPL. **HK** ( $\delta\text{C}/\delta\text{H}$  at about 44.5 /3.67 ppm and 67.1/4.19 ppm) was not detected either in the demethylated HKL, CSL, and ELPL, which further confirmed the instability of **HK** under the demethylation conditions used in this study.

It is worth mentioning that the chemical shifts of **S** and **G** units greatly changed after the demethylation (Fig. S3†), probably due to the cleavage of the ether bonds in the **A**, **B**, and **C** structures. Notably, the signals of **G2** in all four lignins were completely invisible probably due to the demethylation of *ortho*-methoxyl groups (Fig. S3†). Meanwhile, the characteristic signals of ferulate also shifted away, likely due to the removal of the unit during the demethylation (Fig. S3D†).

### Insights into the cleavage of the ether bonds of lignin in the ACLB system

There are different types of ether bonds in lignin, including  $\beta$ -O-4, 4-O-5,  $\alpha$ -O-4 in phenylcoumaran,  $\alpha$ -O- $\gamma$  in resinol, and methyl-O-aryl involving methoxyl groups. The results from the

present and previous studies<sup>43–46</sup> clearly indicate that the ether bonds of lignin except for 4-O-5 can be cleaved in the ACLB system. However, the cleavage mechanisms and the reaction conditions required are dependent on the ether bonds.

**The 4-O-5 ether bond.** The 4-O-5 ether bond should be stable in the ACLB system because the diphenyl ether cannot be cleaved *via* the  $\text{S}_{\text{N}}2$  mechanism, as discussed above (entry 10 in Table 1). In fact, the bond dissociation energy of the 4-O-5 ether bond is 314 kJ mol<sup>-1</sup>, much higher than those of  $\alpha$ -O-4 ( $\alpha$ -O side) and  $\beta$ -O-4 ( $\beta$ -O side) bonds (218 kJ mol<sup>-1</sup> and 289 kJ mol<sup>-1</sup>, respectively).<sup>51</sup>

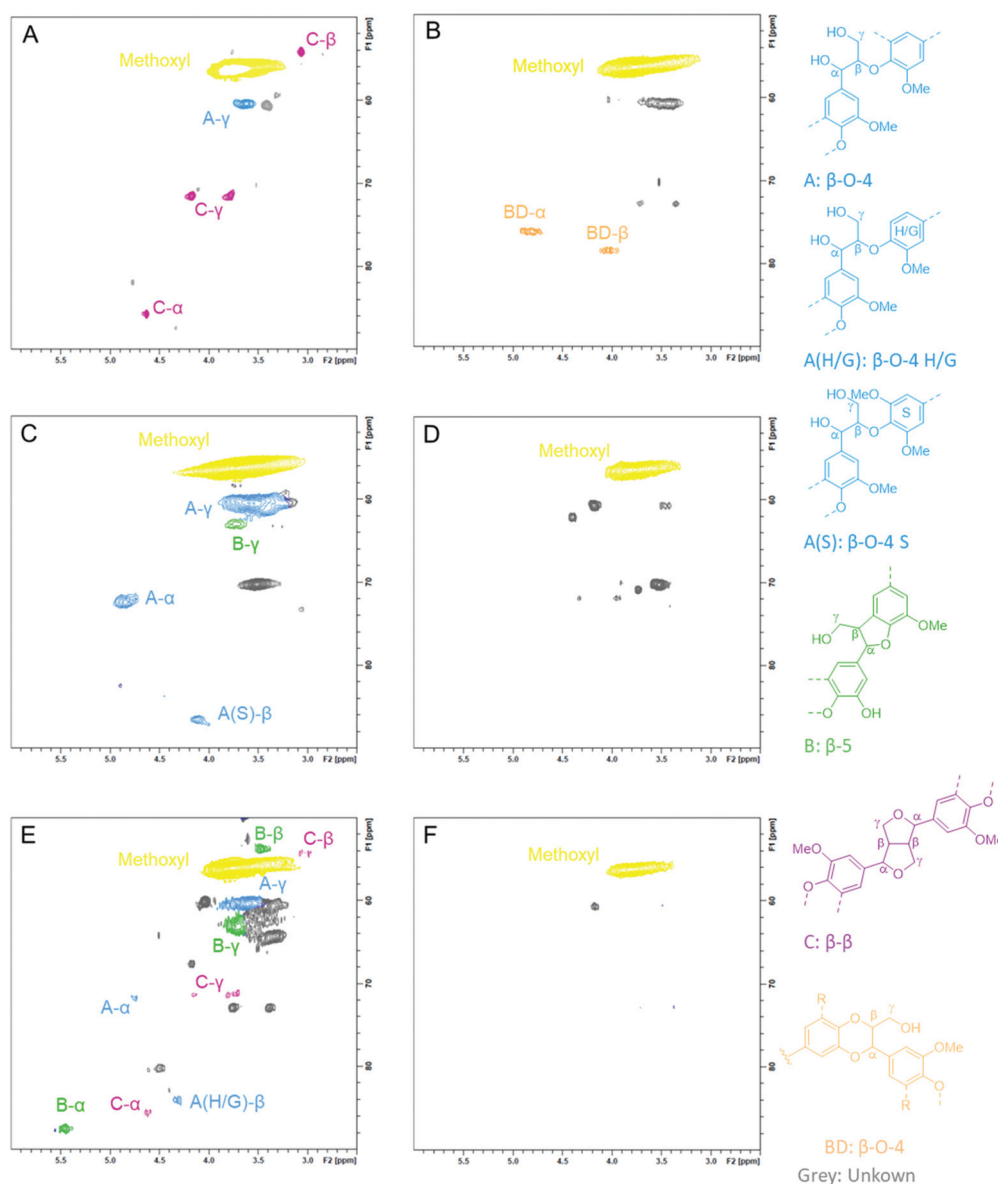
**The methyl-O-aryl ether bond.** It was successfully demonstrated in the present study that the methyl-O-aryl ether can be cleaved in the ACLB system, which leads to a new phenolic hydroxyl group and the elimination of bromomethane.

**The  $\alpha$ -O-4 ether bond in phenylcoumaran and the  $\alpha$ -O- $\gamma$  ether bond in resinol.** The NMR studies of the lignins treated in the ACLB in the present and the previous studies<sup>43–46</sup> revealed that these two types of ether bonds in lignin can be cleaved in the ACLB, even under mild conditions (10–40 mmol L<sup>-1</sup> HCl as a catalyst).<sup>46</sup> The results of THF and 2-methyl THF above (entries 3–6 in Table 1) indicated that the ether bond in the five-membered ring is vulnerable to be cleaved. The  $\alpha$ -O-4 ether bond in phenylcoumaran can be only cleaved from the  $\text{C}_\alpha$  side, not from the aryl side. The  $\alpha$ -O- $\gamma$  ether bond in resinol can be cleaved from both  $\text{C}_\alpha$  and  $\text{C}_\gamma$  sides, while the  $\text{C}_\gamma$  (primary carbon) side should be easier than the  $\text{C}_\alpha$  (secondary carbon) side. Overall, the  $\alpha$ -O- $\gamma$  ether bond in resinol should be easier to be cleaved than the  $\alpha$ -O-4 ether bond in phenylcoumaran.

Based on the reaction mechanism discussed above, the cleavage of these ether bonds would introduce bromine into lignin side chains. Also, some aliphatic hydroxyl groups in lignin could be substituted by bromide in this system. Indeed, a trace amount of bromine was detected in the ACLB-treated lignin. First, the demethylated lignin was analyzed by SEM-EDS, and the  $\text{L}\alpha$  signal of Br at 1.481 keV was observed (Fig. S5†). This is direct evidence of Br existence in the lignin. A negligible amount of Br was also detected in the lignin treated in the LiBr system under milder conditions in a previous study.<sup>43</sup> Second, when the demethylated lignin was oxidized by  $\text{H}_2\text{O}_2$  with  $\text{H}_2\text{SO}_4$  as a catalyst, bromo- and dibromoacetic acids were detected in the oxidation products by GC-MS (Fig. S6†), which were probably from the oxidation of the lignin sidechains. This provided additional evidence of the existence of Br in the treated lignin.

**The  $\beta$ -aryl ether ( $\beta$ -O-4) bond.** It was verified in the previous study<sup>46</sup> that the  $\beta$ -O-4 bond is cleaved *via* the intermediates of benzyl cations and enol ether, leading to the **HK** structure. Meanwhile, some of the  $\beta$ -O-4 bonds, in particular, those in hardwood lignin (**S**-type lignin), are transformed into the **BD** structure, as discussed earlier. The evidence from this study indicated that **BD** could survive in the ACLB system, although it is possible to be cleaved at the  $\text{C}_\alpha$  and  $\text{C}_\beta$  sides of the dioxane ring, as discussed above. It should also be noted that the bond dissociation energy of  $\beta$ -O-4 ether bonds (289 kJ mol<sup>-1</sup>,  $\beta$ -O side) is higher than that of  $\alpha$ -O-4 ether bonds (218 kJ mol<sup>-1</sup>,  $\alpha$ -O





**Fig. 4** Aliphatic region of the HSQC spectra of original and demethylated lignin samples in DMSO- $d_6$ . (A) Original HKL; (B) demethylated HKL; (C) original CSL; (D) demethylated CSL; (E) original ELPL; (F) demethylated ELPL. Reaction conditions: 0.5 g lignin, 6.1 g LiBr (53 wt% in ACLB), 3.9 g water, 1 mL HBr, 100 °C, and 4 h.

side), indicating that the cleavage of  $\beta$ -O-4 ether bonds should be more difficult than that of  $\alpha$ -O-4 ether bonds.<sup>51</sup>

Can the  $\beta$ -O-4 bond be cleaved *via* the  $S_N2$  mechanism? Chemically, it is not impossible but not favorable because the steric hindrance at C $\beta$  (secondary carbon in the middle of the lignin side chain) is very high for the  $S_N2$  substitution. If  $\beta$ -O-4 was primarily cleaved *via* the  $S_N2$  mechanism, **BD** and **HK** would not have been produced, which is certainly not the case and contradicts the results from this and the previous studies. Besides, the  $\beta$ -O-4 cleavage *via* the  $S_N2$  mechanism would have introduced a significant amount of bromine to the C $\beta$  position because  $\beta$ -O-4 is the most abundant ether bonds in lignin, but this was not observed.

## Conclusions

This work demonstrated the ether cleavage and lignin demethylation in acidic concentrated lithium bromide (ACLB) solution. The results revealed that the ACLB could universally cleave (dealkylate) ether compounds except for diaryl ethers. The system was also capable of demethylating lignin model compounds with methoxyl groups (methyl aryl ethers), leading to corresponding phenols. The cleavage of the ether bonds was completed *via* the mechanism of ether oxygen protonation followed by the  $S_N2$  substitution with bromide.

The ACLB was also effective at demethylating real lignin and converting the methoxyl groups into phenolic hydroxyl



groups. Under the conditions investigated, 69–82% of methoxyl groups in four lignins from different sources were demethylated. In addition to demethylation, the ACLB was able to cleave other ether bonds of lignin in  $\beta$ -O-4,  $\beta$ -5, and  $\beta$ - $\beta$  structures except for the 4-O-5 bond in the diphenyl structure. The ether bonds were cleaved *via* the S<sub>N</sub>2 mechanism except for the  $\beta$ -O-4 bond, which was primarily cleaved *via* the benzyl cation and enol ether intermediates, leading to Hibbert's ketones. Some of the  $\beta$ -O-4 structures in hardwood lignin (S-type) were transformed into benzodioxane (BD) structures, which were stable in the ACLB system.

Compared with existing lignin demethylation methods, such as the concentrated HBr method, the ACLB method developed in this study required milder conditions (lower temperature and acid concentration), which would reduce the acid-induced lignin condensation. Besides, ACLB had a better selectivity in converting methoxyl to phenolic hydroxyl groups. A less condensed structure and more phenolic hydroxyl groups would certainly benefit the downstream applications of the demethylated lignin, such as heavy metal adsorbents, antioxidants, lignin-based resin adhesive, and feedstock for dicarboxylic acid production from lignin *via* oxidation.

## Conflicts of interest

There are no conflicts of interest to declare.

## Acknowledgements

This project was supported by USDA NIFA (2018-67009-27902).

## References

- 1 Y. Shao, Q. Xia, L. Dong, X. Liu, X. Han, S. F. Parker, Y. Cheng, L. L. Daemen, A. J. Ramirez-Cuesta, S. Yang and Y. Wang, *Nat. Commun.*, 2017, **8**, 1–9.
- 2 X. Zhou, L. J. Broadbelt and R. Vinu, in *Adv. Chem. Eng.*, Elsevier, 2016, vol. 49, pp. 95–198.
- 3 W. Boerjan, J. Ralph and M. Baucher, *Annu. Rev. Plant Biol.*, 2003, **54**, 519–546.
- 4 M. Jablonsky, M. Botkova and J. Kosinkova, *Cellul. Chem. Technol.*, 2015, **49**, 165–168.
- 5 H. H. Nimz, D. Robert, O. Faix and M. Nemr, *Holzforschung*, 1981, **35**, 16–26.
- 6 R. Vanholme, B. Demedts, K. Morreel, J. Ralph and W. Boerjan, *Plant Physiol.*, 2010, **153**, 895–905.
- 7 K. M. Holtman, H. Chang and J. F. Kadla, *J. Agric. Food Chem.*, 2004, **52**, 720–726.
- 8 A. Guerra, I. Filpponen, L. A. Lucia and D. S. Argyropoulos, *J. Agric. Food Chem.*, 2006, **54**, 9696–9705.
- 9 K. M. Holtman, H. Chang, H. Jameel and J. F. Kadla, *J. Wood Chem. Technol.*, 2006, **26**, 21–34.
- 10 S. Wang, B. Ru, H. Lin, W. Sun and Z. Luo, *Bioresour. Technol.*, 2015, **182**, 120–127.
- 11 D. E. Bland and A. F. Logan, *Biochem. J.*, 1965, **95**, 515–520.
- 12 A. E. Kazzaz, Z. H. Feizi and P. Fatehi, *Green Chem.*, 2019, **21**, 5714–5752.
- 13 A. M. Olsson and L. Salmén, *Nord. Pulp Pap. Res. J.*, 1997, **12**, 140–144.
- 14 X. Pan, J. F. Kadla, K. Ehara, N. Gilkes and J. N. Saddler, *J. Agric. Food Chem.*, 2006, **54**, 5806–5813.
- 15 I. Sumerskii, T. Zweckmair, H. Hettegger, G. Zinovyev, M. Bacher, T. Rosenau and A. Potthast, *RSC Adv.*, 2017, **7**, 22974–22982.
- 16 J. Li, J. Zhang, S. Zhang, Q. Gao, J. Li and W. Zhang, *Polymers*, 2017, **9**, 428–445.
- 17 H. Schroeder, Method For Recovering And Using Lignin In Adhesive Resins By Extracting Demethylated Lignin, *US Pat.*, US5026808A, 1991.
- 18 H. Wang, T. L. Eberhardt, C. Wang, S. Gao and H. Pan, *Polymers*, 2019, **11**, 1771–1787.
- 19 S. Wu and H. Zhan, *Cellul. Chem. Technol.*, 2001, **35**, 253–262.
- 20 Y. Song, Z. Wang, N. Yan, R. Zhang and J. Li, *Polymers*, 2016, **8**, 209.
- 21 B. Wang, J. Wen, S. Sun, H. Wang, S. Wang, Q. Liu, A. Charlton and R.-C. Sun, *Ind. Crops Prod.*, 2017, **108**, 72–80.
- 22 A. L. Pometto III, J. B. Sutherland and D. L. Crawford, *Can. J. Microbiol.*, 1981, **27**, 636–638.
- 23 M. L. Álvarez-Rodríguez, C. Belloch, M. Villa, F. Uruburu, G. Larriba and J. R. Coque, *FEMS Microbiol. Lett.*, 2003, **220**, 49–55.
- 24 S. H. Champion and I. D. Suckling, *Appita J.*, 1998, **51**, 209–212.
- 25 T. R. Filley, G. D. Cody, B. Goodell, J. Jellison, C. Noser and A. Ostrofsky, *Org. Geochem.*, 2002, **33**, 111–124.
- 26 S. Zhao and M. M. Abu-Omar, *Macromolecules*, 2017, **50**, 3573–3581.
- 27 Q. Mei, H. Liu, X. Shen, Q. Meng, H. Liu, J. Xiang and B. Han, *Angew. Chem., Int. Ed.*, 2017, **56**, 14868–14872.
- 28 N. A. David, *Annu. Rev. Pharmacol.*, 1972, **12**, 353–374.
- 29 J. Gierer, *Wood Sci. Technol.*, 1980, **14**, 241–266.
- 30 TAPPI, T 209 su-72 Methoxyl Content of Pulp and Wood, *TAPPI Test Methods*, TAPPI Press: Atlanta, Georgia, 1972.
- 31 F. Kačik, D. Kačiková, T. Bubenikova and V. Velková, *Drewno*, 2004, **47**, 113–119.
- 32 V. Viswanatha and G. S. K. Rao, *J. Chem. Soc., Perkin Trans. 1*, 1974, 450–453.
- 33 H. Lee, X. Feng, M. Mastalerz and S. J. Feakins, *Org. Geochem.*, 2019, **136**, 103894.
- 34 K. Sawamura, Y. Tobimatsu, H. Kamitakahara and T. Takano, *ACS Sustainable Chem. Eng.*, 2017, **5**, 5424–5431.
- 35 S. Zhao and M. M. Abu-Omar, *Biomacromolecules*, 2015, **16**, 2025–2031.
- 36 P. P. Kulkarni, R. B. Mane, U. V. Desai and P. P. Wadgaonkar, *J. Chem. Res., Synop.*, 1999, 394–395.
- 37 M. E. Jung and M. A. Lyster, *J. Org. Chem.*, 1977, **42**, 3761–3764.
- 38 Y. Song, Z. Wang, N. Yan, R. Zhang and J. Li, *Polymers*, 2016, **8**, 209–223.
- 39 M. Ferhan, N. Yan and M. Sain, *J. Chem. Eng. Process Technol.*, 2013, **4**, 1000160.



- 40 X. Li, J. He and Y. Zhang, *J. Org. Chem.*, 2018, **83**, 11019–11027.
- 41 B. G. Harvey, A. J. Guenther, W. W. Lai, H. A. Meylemans, M. C. Davis, L. R. Cambrea, J. T. Reams and K. R. Lamison, *Macromolecules*, 2015, **48**, 3173–3179.
- 42 J. Tian, C. Yi, H. Fang, D. Sang, Z. He, J. Wang, Y. Gan and Q. An, *Tetrahedron Lett.*, 2017, **58**, 3522–3524.
- 43 N. Li, X. Pan and J. Alexander, *Green Chem.*, 2016, **18**, 5367–5376.
- 44 C. G. Yoo, S. Zhang and X. Pan, *RSC Adv.*, 2017, **7**, 300–308.
- 45 X. Yang, N. Li, X. Lin, X. Pan and Y. Zhou, *J. Agric. Food Chem.*, 2016, **64**, 8379–8387.
- 46 N. Li, Y. Li, C. G. Yoo, X. Yang, X. Lin, J. Ralph and X. Pan, *Green Chem.*, 2018, **20**, 4224–4235.
- 47 X. Pan, D. Xie, R. W. Yu, D. Lam and J. N. Saddler, *Ind. Eng. Chem. Res.*, 2007, **46**, 2609–2617.
- 48 G. Pruckmayr and T. K. Wu, *Macromolecules*, 1978, **11**, 662–668.
- 49 P. A. Delaney, R. A. W. Johnstone and I. D. Entwistle, *J. Chem. Soc., Perkin Trans. 1*, 1986, 1855–1860.
- 50 B. H. Kwant, *J. Labelled Compd. Radiopharm.*, 1980, **17**, 841–859.
- 51 J. He, C. Zhao and J. A. Lercher, *J. Am. Chem. Soc.*, 2012, **134**, 20768–20775.
- 52 C. Zhu, J. Cao, X. Zhao, T. Xie, J. Ren and X. Wei, *J. Energy Inst.*, 2019, **92**, 74–81.
- 53 J. A. Duffy and M. D. Ingram, *Inorg. Chem.*, 1978, **17**, 2798–2802.
- 54 S. Sen, J. D. Martin and D. S. Argyropoulos, *ACS Sustainable Chem. Eng.*, 2013, **1**, 858–870.
- 55 X. Pan and Y. Sano, *Holzforschung*, 1999, **53**, 590–596.
- 56 J. Li, G. Henriksson and G. Gellerstedt, *Bioresour. Technol.*, 2007, **98**, 3061–3068.
- 57 F. Chen, Y. Tobimatsu, D. Havkin-Frenkel, R. A. Dixon and J. Ralph, *Proc. Natl. Acad. Sci. U. S. A.*, 2012, **109**, 1772–1777.
- 58 J. Ralph, C. Lapierre, J. M. Marita, H. Kim, F. Lu, R. D. Hatfield, S. Ralph, C. Chapple, R. Franke and M. R. Hemm, *Phytochemistry*, 2001, **57**, 993–1003.
- 59 J. Ralph, C. Lapierre, F. Lu, J. M. Marita, G. Pilate, J. Van Doorselaere, W. Boerjan and L. Jouanin, *J. Agric. Food Chem.*, 2001, **49**, 86–91.
- 60 P. J. Deuss, M. Scott, F. Tran, N. J. Westwood, J. G. de Vries and K. Barta, *J. Am. Chem. Soc.*, 2015, **137**, 7456–7467.

